

# Measuring neutron capture rates on ILL-produced unstable isotopes ( $^{147}\text{Pm}$ , $^{171}\text{Tm}$ and $^{204}\text{Tl}$ , and plans for $^{79}\text{Se}$ and $^{163}\text{Ho}$ ) for nucleosynthesis studies

J. Lereendegui-Marco<sup>1,\*</sup>, C. Guerrero<sup>1</sup>, C. Domingo-Pardo<sup>2</sup>, A. Casanovas<sup>3</sup>, R. Dressler<sup>4</sup>, S. Halfon<sup>5</sup>, S. Heinitz<sup>4</sup>, N. Kivel<sup>4</sup>, U. Köster<sup>6</sup>, M. Paul<sup>7</sup>, D. Schumann<sup>4</sup>, M. Tessler<sup>7</sup>, and The n\_TOF Collaboration<sup>8</sup>

<sup>1</sup> *Universidad de Sevilla, Sevilla, Spain*

<sup>2</sup> *Instituto de Física Corpuscular, Paterna, Spain*

<sup>3</sup> *Universitat Politècnica de Catalunya, Barcelona, Spain*

<sup>4</sup> *Paul Scherrer Institut, Villigen, Switzerland*

<sup>5</sup> *Soreq NRC, Yavne, Israel*

<sup>6</sup> *Institut Laue-Langevin, Grenoble, France*

<sup>7</sup> *Racah Institute of Physics, Hebrew University, Jerusalem, Israel*

<sup>8</sup> [www.cern.ch/ntof](http://www.cern.ch/ntof)

**Abstract.** Neutron capture cross sections are among the main inputs for nucleosynthesis network calculations. Although well known for the majority of the stable isotopes, this quantity is still unknown for most of the unstable isotopes of interest. A recent collaboration between ILL, PSI, U. Sevilla and IFIC aims at producing the isotopes of interest at ILL, preparing suitable targets at PSI, and measuring their capture cross sections at facilities such as n\_TOF/CERN, LiLiT and the Budapest Research Reactor (BRR). This work is focused on the description of the different beams and techniques and shows some highlights of the preliminary results of the capture measurements on  $^{171}\text{Tm}$ ,  $^{147}\text{Pm}$  and  $^{204}\text{Tl}$ , along with the future plans for  $^{79}\text{Se}$  and  $^{163}\text{Ho}$ .

## 1 Introduction and motivations

Nucleosynthesis in star cores by means of fusion reactions is responsible just for the generation of elements up to iron. Heavier elements are produced in several processes driven mainly by neutron capture reactions in stellar sites, half of them being synthesized in the slow neutron capture process (s-process). This process takes place in the He-burning layers of low-mass asymptotic giant branch (AGB) stars and during the He- and C-burning phases of massive stars. The corresponding nucleosynthesis studies involve detailed stellar modeling, constrained by spectroscopic observations and meteoritic stardust grains, in which reliable information on the nuclear physics part, in particular on the basic nuclear data such as half-lives and neutron capture ( $n,\gamma$ ) cross sections, constitute an essential ingredient [1, 2]. A better knowledge of neutron capture rates in stars is specially relevant for the case of certain unstable isotopes acting as branching points since they open new branches in the

---

\*e-mail: [jlereendegui@us.es](mailto:jlereendegui@us.es)

s-process path due to the competition between  $\beta$ -decay and neutron capture, which depends on the neutron density, the Maxwellian Averaged Cross Section (MACS) and the mean thermal neutron velocity, i.e. the neutron energy distribution at a given temperature. In addition, both half-life and  $(n,\gamma)$  reaction rates depend in some case on the temperature of the stellar site because of the population of some levels above the ground state. This dependence has a sizable effect on s-process abundance calculations for some isotopes [3] and cannot be measured, so measurements have to be combined with models [4].

The measurement of the branch-point isotopes presents several challenges and for this reason just few measurements have been performed. The difficulties, prospects and new techniques to enable measurements that are not feasible up to date, are discussed in detail in Ref. [5]. However, several isotopes, listed in Ref. [1] can be measured with the current beams and techniques. Among them, only  $^{63}\text{Ni}$  [6, 7] and  $^{151}\text{Sm}$  [8] have been measured by time-of-flight (ToF) so far, and just a few more by activation (see Ref. [1] for the details). In this context, a collaboration was established between the Institut Laue-Langevin (ILL), the Paul Scherrer Institut (PSI) and University of Sevilla within the EU FP7 projects NEUTANDALUS and CHANDA for measuring by time-of-flight the capture cross section of the branching point isotopes  $^{147}\text{Pm}$ ,  $^{171}\text{Tm}$  and  $^{204}\text{Tl}$  at the n\_TOF facility. Additional measurements of the first two isotopes were performed by activation at the LiLiT facility at SARAF (Israel), featuring a high intensity quasi-Maxwellian spectrum ( $kT=42$  keV), and will be done soon in the Budapest Research Reactor (BRR) by means of the PGAA technique with a cold neutron beam. Section 2 of this paper focuses in the production of high quality unstable targets. In Section 3 we describe complementary neutron beams and techniques to measure unstable isotopes. Last, in Section 4 some highlights of the preliminary results are presented.

## 2 Isotope production and target preparation

The radioactive isotopes in this work were produced by irradiating stable pellets of  $^{146}\text{Nd}$  ( $^{146}\text{Nd}(n,\gamma)^{147}\text{Nd} \rightarrow ^{147}\text{Pm} + \beta^-$ ),  $^{170}\text{Er}$  ( $^{170}\text{Er}(n,\gamma)^{171}\text{Er} \rightarrow ^{171}\text{Tm} + \beta^-$ ) and  $^{203}\text{Tl}$  ( $^{203}\text{Tl}(n,\gamma)^{204}\text{Tl}$ ) respectively, in the V4 beam tube of the ILL high flux reactor in Grenoble, France for eight weeks with an average neutron flux ranging from 0.8 to  $1.3 \times 10^{15}$  n/cm<sup>2</sup>/s. The irradiated pellets containing  $^{147}\text{Pm}$  and  $^{171}\text{Tm}$  were chemically purified at PSI in Switzerland and high quality targets (22 mm diameter), suited for capture experiments, were prepared through electroplating into 5  $\mu\text{m}$  thick aluminum backings. On the other hand, the produced  $^{204}\text{Tl}$  target was left inside the quartz ampule used for the irradiation due to its prohibitive dose rate. The total masses of the targets already produced within this project are listed in Table 1 along with the masses and enrichment of the stable seeds irradiated at ILL. For all the details on the radiochemistry and sample manufacturing the reader is referred to Ref. [9].

Isotope (mass)	Sample production		(n, $\gamma$ ) measurements		
	Seed/Enrichment (mass)		n_TOF	LiLiT	BRR
$^{147}\text{Pm}$ (85 $\mu\text{g}$ )	$^{146}\text{Nd}_2\text{O}_3$ / 98.8% (98.2 mg)		EAR2	Yes	Fall 2017
$^{171}\text{Tm}$ (3.48 mg)	$^{170}\text{Er}_2\text{O}_3$ / 98.1% (238 mg)		EAR1	Yes	Fall 2017
$^{204/203}\text{Tl}$ (9/216 mg)	$^{203}\text{Tl}_2\text{O}_3$ / 99.5% (251 mg)		EAR1	No*	Not planned

**Table 1.** Measured s-process branching isotopes: final masses, irradiated seeds and facilities involved in the measurements. \* $^{205}\text{Tl}$  is stable and cannot be measured in activation experiments.

### 3 Neutron beams and experimental techniques

The successful collaboration between institutes allowed us to measure high quality unstable targets using complementary beams and techniques. This section describes briefly the n\_TOF facility at CERN, the LiLiT facility at SARAF and the PGAA measurements at the Budapest Research Reactor. The facilities involved in each measurement are presented in Table 1.

#### 3.1 Time-of-flight measurements at n\_TOF-CERN

The pulsed white neutron beam at n\_TOF is generated through spallation of 20 GeV/c protons from the CERN Proton Synchrotron (CPS) impinging on a thick lead target. Each proton bunch contains, on average,  $7 \cdot 10^{12}$  protons with a time distribution of  $\sigma=7$  ns and an average repetition rate of 0.17 Hz. The spallation neutrons, with energies in the MeV-GeV range, are partially moderated in the water cooling and moderation layers around the lead target to expand their energies from thermal to GeV and travel towards the experimental areas along two beam lines: EAR1 [10] at 185 m (horizontal) and EAR2 [11] at 19 m (vertical). At n\_TOF, high energy resolution measurements of point-wise cross-sections are performed by means of the time-of-flight technique.

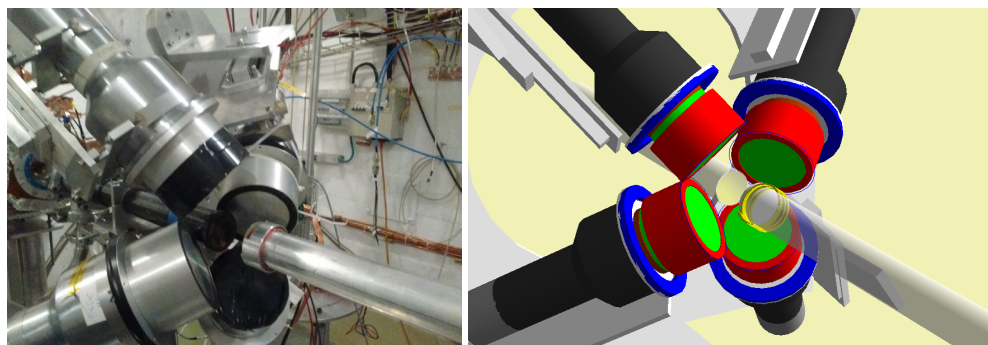


**Figure 1.** *Left: Array of 4 C<sub>6</sub>D<sub>6</sub> detectors used to detect the  $\gamma$ -ray cascades emitted in the neutron capture on the unstable isotope. Right: Geometry model implemented in Geant4 to simulate the response of the detection set-up.*

Radiative capture at n\_TOF is measured with two different detection systems. One can choose to detect the full cascade using the  $4\pi$  BaF<sub>2</sub> Total Absorption Calorimeter (TAC) [12], or just one of the  $\gamma$ -rays of the cascade by means of the Total Energy Detection technique [13], with an array of four low neutron sensitivity C<sub>6</sub>D<sub>6</sub> detectors [14]. The array of four C<sub>6</sub>D<sub>6</sub> were chosen for the measurements of <sup>147</sup>Pm (n\_TOF-EAR2), <sup>171</sup>Tm and <sup>204</sup>Tl (n\_TOF-EAR1) mainly because they suffer significantly less from the so-called  $\gamma$ -flash than the TAC, due to their fast response and reduced mass, thus allowing us to measure up to the required neutron energy. The set-up of four detectors used in the measurements at n\_TOF-EAR1 is shown in the left panel of Figure1. The right panel shows the corresponding geometry implemented in the Monte Carlo simulation with the Geant4 toolkit [15] used for assessing the detection efficiency.

### 3.2 MACS activation measurements at LiLiT

The Liquid Lithium Target (LiLiT) [16] installed at the SARAF facility (Israel) provides the most intense quasi-Maxwellian neutron beam worldwide. The SARAF accelerator provides a proton beam of 1-2 mA with an energy of 1.935 keV (just above the threshold of the  ${}^7\text{Li}(p,n)$  reaction) that is driven into a thin (1.5 mm) liquid lithium layer, hence providing the quasi-Maxwellian neutron energy distribution (see Ref.[17] for details). Figure 2 shows a sketch of the Lithium target (left panel) and the experimental flux compared to a Maxwellian distribution at  $kT = 42.3$  keV (right panel). At LiLiT, Maxwellian Averaged Cross Sections (MACS) are measured via the activation technique. The targets ( ${}^A_Z\text{X}$ ) are exposed to the neutron beam and the number of capture reactions ( ${}^A_Z\text{X} + n \rightarrow {}^{A+1}_Z\text{Y}$ ) is determined from the number of  ${}^{A+1}_Z\text{Y}$  nuclei produced. Assuming that the  ${}^{A+1}_Z\text{Y}$  isotope is radioactive, the number of unstable nuclei is quantified using a Ge detector looking at the associated emission of  $\gamma$ -rays. In this case, the MACS of  ${}^{197}\text{Au}$  serves as a reference.

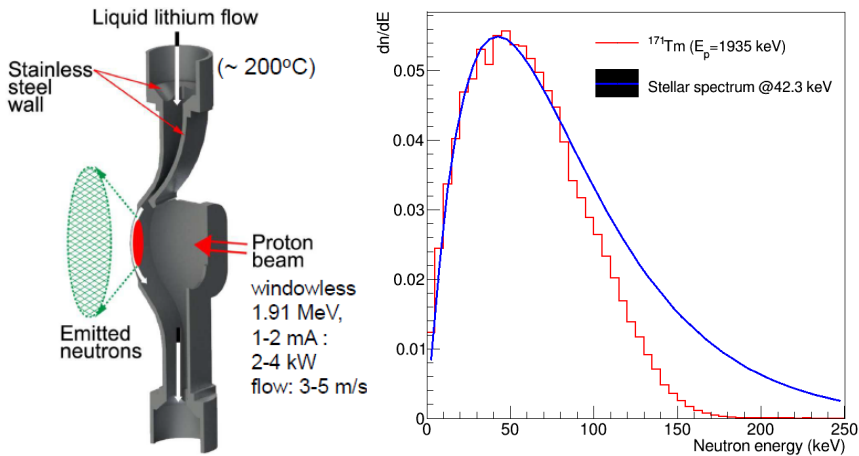


**Figure 2.** Left: Sketch of the liquid lithium neutron source at SARAF. Right: Comparison between the simulated neutron flux at LiLiT and the theoretical Maxwellian neutron spectrum at 42.3 keV

### 3.3 Thermal point via Prompt Gamma Activation Analysis at BRR

The Time-of-Flight and MACS measurements will be complemented by the end of 2017 with a thermal capture cross section measurement at the Budapest Research Reactor (BRR) by means of Prompt Gamma Activation Analysis (PGAA) [18]. The BRR presents different neutron beam lines extracted from a experimental thermal reactor. One of them features a cold neutron beam (average energy 12 meV,  $kT = 140$  K) and is equipped with a PGAA experimental set-up. This technique is a nuclear analysis method based on the detection of the prompt gamma radiation released in the radiative neutron capture reaction to identify and quantify the isotopic content of samples. However, we will use it to extract the thermal capture cross section by irradiating the sample of interest, inducing capture reactions and detecting the subsequent prompt gamma rays with a BGO guarded Compton-suppression HPGe detector.

## 4 Results

A detailed description of the data reduction towards the final results is out of the scope of this work. However, in this section we will summarize the main features of each measurement and show some highlights of the obtained results.

### 4.1 $^{171}\text{Tm}$

The  $^{171}\text{Tm}(n,\gamma)$  experiment at n\_TOF-EAR1, was carried out at the end of 2014 and became the first time-of-flight measurement of this cross-section except for a test done in LANL. The capture reactions in this measurement were registered as a function of the time-of-flight (i.e. neutron energy) via the detection of one  $\gamma$ -ray per cascade, following the principles of the Total Energy Detection technique. Besides the  $^{171}\text{Tm}$  sample, different ancillary measurements were also performed to determine the level of the different background components as well as for normalization purposes. Among the first ones, the sample activity background (mainly coming from the 0.4 GBq  $^{170}\text{Tm}$ ) is clearly dominant over the capture as one can see in the top panel of Figure 3. The beam-dependent backgrounds, generated by neutrons and in-beam photons are assessed by measuring an empty replica of the  $^{171}\text{Tm}$  target backings and a lead sample, respectively. The level of the total background is shown as a red curve in Figure 3. Above this background resonances can be identified up to 700 eV (see inset in Figure 3).

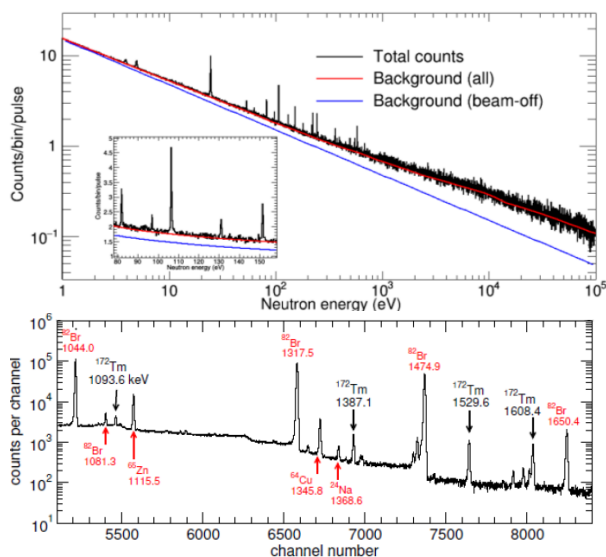


**Figure 3.** *Top: Distribution of counts as function of the neutron energy during the  $^{171}\text{Tm}(n,\gamma)$  experiment at n\_TOF. The main figure illustrates the dominant beam-off background from the activity of the target, while the inset shows how resonances are well resolved even on top of such a high background. Bottom: Energy spectrum registered with the HPGe system at LiLiT in the energy range of the  $^{172}\text{Tm}$  decay characteristic lines.*

To extract the neutron capture yield,  $Y_{exp}(E_n) = \frac{1}{f_{SRM}} \cdot \frac{C_w(E_n) - B_w(E_n)}{\Phi(E_n)\epsilon}$ , the background-subtracted counting rate per pulse  $C_w - B_w$  (Left panel of Figure 3) is divided by the neutron flux per pulse  $\Phi$  of n\_TOF-EAR1 [19] and the efficiency, which by construction of the TED, is numerically equal to

the cascade energy  $\varepsilon = S_n + E_n$ . In order to achieve this equality a mathematical manipulation of the detector response, based in accurate MC simulations (Figure1), known as Pulse Height Weighting Technique (PHWT), has to be applied [20].  $f_{SRM}$  represents the absolute normalization factor obtained through the Saturated Resonance Method from the accurately known value of the saturated plateau of the first resonance in the  $^{197}\text{Au}(n,\gamma)$  ancillary measurement.

The 28 s-wave resonances in the experimental capture yield have been analysed and parameterized using the Bayesian R-matrix analysis code SAMMY [21] and extracting individual resonance parameters for the first time in history. From the statistical analysis of the resonances we can conclude that the TALYS prediction clearly overestimates the  $^{171}\text{Tm}$  capture cross section in terms of both resonance strength and resonance density. These average parameters affect the cross-section in the keV range and thus a clear reduction of the MACS compared to TALYS prediction is expected.

The activation experiment at the SARAF-LiLiT facility was carried out in spring 2016. The cross section of  $^{171}\text{Tm}$  was measured in reference to that of  $^{197}\text{Au}$ , for which a target of same diameter in an identical Al holder was irradiated under the same conditions. The number of  $(n,\gamma)$  reactions on  $^{171}\text{Tm}$  and  $^{197}\text{Au}$  was determined from the activity of  $^{172}\text{Tm}$  (2.65 d) and  $^{198}\text{Au}$  (2.70 d) measured with a statistical accuracy better than 1% with a HPGe detector shielded using Pb absorbers to attenuate the high-intensity low-energy photons (Bremsstrahlung, X- and  $\gamma$ -rays) from the  $^{171}\text{Tm}$ . Four different  $\gamma$ -ray lines of the  $^{172}\text{Tm}$ , shown in the bottom panel of Figure 3, were analysed and the obtained activities are in agreement within the uncertainty in the transition intensities. The resulting Maxwellian Averaged Cross Section (MACS) is calculated as a function of the number of produced  $^{172}\text{Tm}$  ( $N_{act}^{Tm}$ ) and  $^{198}\text{Au}$  ( $N_{act}^{Au}$ ) nuclei, and the  $^{197}\text{Au}$  reference MACS. The preliminary results indicate a situation compatible with what was found in the eV region at n\_TOF. The MACS in the keV region is significantly smaller (between a factor 2 and 5 lower) than the KaDoNiS, TALYS and JEFF values. It is also smaller than the only experimental value of 350 mb by Reifarth et al. [22]. In order to ensure the reliability of the result, a  $^{169}\text{Tm}$  target was measured under similar conditions, and the result was found to agree within the uncertainties with the values from previous measurements.

The final result of this work and the astrophysical implications of the reduced MACS values can be found in Ref. [24].

## 4.2 $^{147}\text{Pm}$

The  $^{147}\text{Pm}(n,\gamma)$  experiment at n\_TOF-EAR2 was carried out in spring 2015. Up to date this capture measurement features the smallest mass (85  $\mu\text{g}$ ) ever measured at the n\_TOF facility. The mass was unexpectedly small due to the deviations in the assumed value for the thermal capture cross section of  $^{146}\text{Nd}$  (seed irradiated at ILL). For this reason n\_TOF-EAR2 was chosen over EAR1, featuring the highest instantaneous neutron flux among time-of-flight facilities worldwide [25]. The small mass just allowed to clearly measure the three largest resonances (see left panel of Figure 4) and identify ten additional resonances up to few hundreds of eV, not enough to perform any kind of statistical analysis or extract any MACS value.

A direct MACS measurement was performed at LiLiT in similar conditions than for  $^{171}\text{Tm}$ . The experimental setup and analysis technique are the same (with slightly higher proton beam energy of 1940 keV instead of 1935 keV) described for the first isotope. The main difference for the capture in  $^{147}\text{Pm}$  is that two states with different half-lives are populated: the ground state  $^{148}\text{Pm}$  (5.4 d) and the metastable  $^{148m}\text{Pm}$  (41.5 d), whose decay is shown in the right panel of Figure 4; each of them contributing to a fraction of the total cross section. The comparison of the preliminary results with the data of Reifarth et al. (the only previous measurement available) indicate a 1.5-2 times higher cross section. The new data also indicate quite different cross section values for neutron capture going to the ground and isomer state of  $^{148}\text{Pm}$ , contrary to what was found by Reifarth et al. [26].



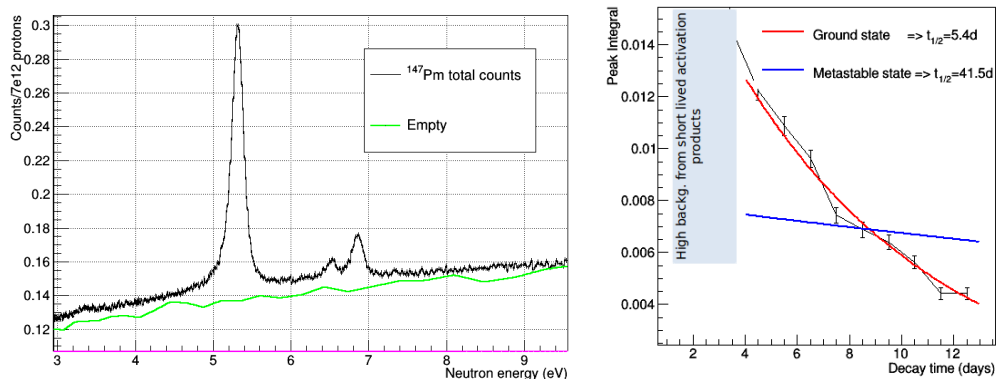


**Figure 4.** Left: Counting rate per pulse as a function of the neutron energy measured in the  $^{147}\text{Pm}(n,\gamma)$  at n\_TOF-EAR2 where one can see the first capture resonances on top of the background. Right: Evolution with time of the peak integral of the 1014 keV  $\gamma$ -ray from the  $^{148}\text{Pm}$  (g.s.) decay fitted to the expected half-life.

### 4.3 $^{204}\text{Tl}$

The  $^{203-204}\text{Tl}(n,\gamma)$  campaign took place at n\_TOF-EAR1, with the same experimental setup with four  $\text{C}_6\text{D}_6$  detectors used for the capture measurement on  $^{171}\text{Tm}$ . The high radioactivity of the sample (400 GBq) and its high  $\beta$  decay Q-value (763 keV) forced us to include a 2 mm lead shielding on the detectors to reduce the related background and avoid any shift in the gain of the detectors, observed in previous measurements with highly radioactive targets, such as  $^{241}\text{Am}$  [27]. In addition, a position sensitive scanner was designed to determine the position of the partially disaggregated pellet inside the quartz ampoule. Since the largest fraction of the sample composition was  $^{203}\text{Tl}$ , a pure sample of this isotope was also measured to identify the contribution of  $^{204}\text{Tl}$ . The right panel of Figure 5 shows preliminary results of the resonance analysis of the  $^{203-204}\text{Tl}$  (black) and  $^{203}\text{Tl}$  (blue) yields performed with the SAMMY code in the energy range from 0.6 to 2.4 keV. The highlighted resonances are the

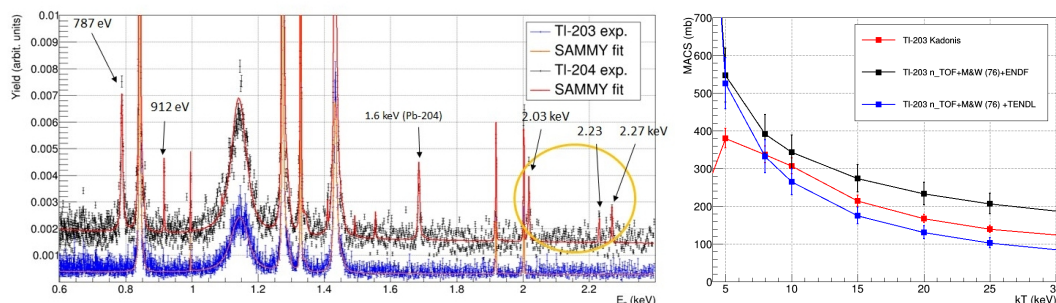


**Figure 5.** Left: Radiative capture yields of  $^{203-204}\text{Tl}$  (black) and  $^{203}\text{Tl}$  (blue) samples fitted with the SAMMY code. The highlighted resonances are the first resonances of  $^{204}\text{Tl}$ . Right: Effect in the MACS at different  $kT$  of the preliminary  $^{203}\text{Tl}(n,\gamma)$  cross section measured up to 16 keV at n\_TOF-EAR1 (see text for details).

first ever observed ones of the  $^{204}\text{Tl}(n,\gamma)$  cross section. In the right panel of the same figure one can see the effect in the MACS at different kT of the preliminary  $^{203}\text{Tl}(n,\gamma)$  cross section measured in this work (up to 16 keV) combined with previous data from Macklin and Winters [28] (from 16 to 35 keV) and ENDF or TENDL at higher energies. From this figure, it is clear that the MACS at kT = 5 keV shows a large increase compared to the value proposed in KaDoNis due to the newly observed resonances.

## 5 Summary and outlook

A better knowledge of the neutron capture rates of the branching point isotopes at stellar temperatures is critical for the s-process nucleosynthesis studies. However, measurements with the current beams and techniques require high mass and sample purity. In this context, a successful collaboration between ILL, PSI, n\_TOF, LiLiT and U. of Sevilla has been established to produce high quality and almost isotopically pure targets and combine time-of-flight measurements in a white neutron beam with activation in a quasi-stellar spectra and prompt gamma activation at thermal energy to obtain complementary results. This manuscript describes the experimental techniques and the status of the results of the already measured isotopes:  $^{171}\text{Tm}$ ,  $^{147}\text{Pm}$  and  $^{204}\text{Tl}$ .

This project includes two future measurements of s-process branching isotopes at n\_TOF-CERN. First,  $^{79}\text{Se}$ , which is specially relevant since the branching at A=69 it is particularly well suited for determining the thermal conditions of the stellar environment. This measurement was already approved in 2014 by the Isolde and n\_TOF Committee at CERN (INTC) [29] and it is foreseen for 2018. Another very interesting isotope,  $^{163}\text{Ho}$ , is key in the understanding of the Dy/Ho branching. The isotope  $^{163}\text{Dy}$  is stable, but it could  $\beta$  decay to  $^{163}\text{Ho}$  at high temperature in the stellar plasmas and then the neutron capture in  $^{163}\text{Ho}$  would be opened. A total of 7.5 mg of this isotope have been produced by ILL for the HOLMES collaboration [30] which aims at measuring the electron neutrino mass by accurately determining the end point of the EC decay of this isotope with a calorimeter. If the activities of the HOLMES experiment allowed to borrow a fraction of the material, the measurement at n\_TOF-EAR2 would be proposed to the INTC soon and performed in 2018.

## Acknowledgments

The authors acknowledge financial support by University of Sevilla via the VI PPIT-US program, the Spanish FPA2013-45083-P and FPA2014-53290-C2-2-P projects, and the EC FP7 projects NeutAndalus (Grant No. 334315) and CHANDA (Grant No. 605203). The SARAF-LiLiT experiment was supported by the Pazi Foundation (Israel) and Israel Science Foundation (Grant No. 1387/15).

## References

- [1] F. Käppeler, R. Gallino, S. Bisterzo, and W. Aoki, *Rev. Mod. Phys.* **83**, 157 (2011)
- [2] R. Reifarh, C. Lederer and F. Käppeler, *J. Phys. G: Nucl. Part. Phys.* **41**, 053101 (2014)
- [3] J. Avila et al., *Astrop. J.* **768**, 1 (2013)
- [4] T. Rauscher, *Astrop. J. Letters* **755**, 1 (2012)
- [5] C. Guerrero et al, *Eur. Phys. J. A* **53**, 87 (2017)
- [6] C. Lederer et al., *Phys. Rev. Lett.* **110**, 022501 (2013) and *Phys. Rev. C* **89**, 025810 (2014)
- [7] M. Weigand et al., *Phys. Rev. C* **92**, 045810 (2015)
- [8] U. Abbondanno et al., *Phys. Rev. Lett.* **93**, 161103 (2004)



- [9] S. Heinitz et al., *Radiochim. Acta* (2017); aop
- [10] C. Guerrero et al., *Eur. Phys. J. A* **49**, 27(2013)
- [11] C. Weiss et al., *Nucl. Instrum. and Meth. A* **799**, 90–98 (2015)
- [12] C. Guerrero et al., *Nucl. Instrum. Methods A* **608**, 424 (2009)
- [13] R.L. Macklin, J.H. Gibbons, *Phys. Rev.* **159**, 1007 (1967)
- [14] R. Plag et al., *Nucl. Instrum. and Meth. A* **496**, 425–436 (2003)
- [15] J. Allison et al., *IEEE Trans. on Nucl. Sci.* **53**, Issue:1, 270-278 (2006)
- [16] S. Halfon, et al., *Rev. Sci. Instrum.* **85**, 056105 (2014)
- [17] W. Ratynski and F. Käppeler, *Phys. Rev. C* **37**, 595 (1988)
- [18] T. Belgya, *Physics Procedia*, **31**, 99-109 (2012)
- [19] M. Barbagallo et al., (The n\_TOF Collaboration), *EPJ A* **49**, 156 (2013)
- [20] U. Abbondanno et al., *Nucl. Instrum. and Meth. A* **521**, 454–467 (2004)
- [21] N. M. Larson, ORNL/TM-9179/R8, ORNL, Oak Ridge, TN, USA (2008)
- [22] R. Reifarth et al., *Nuclear Physics A* **718**, 478 (2003)
- [23] R. Macklin, *Nucl. Sci. Eng.* **82**, 143 (1982)
- [24] C. Guerrero et al., *Neutron capture on the s-process branching point  $^{171}\text{Tm}$  via time-of-flight and activation* (Submitted to PRL)
- [25] J. Lerendegui-Marco, S. Lo Meo, C. Guerrero et al. *Eur. Phys. J. A* **52**, 100 (2016)
- [26] R. Reifarth et al., *The Astrophysical Journal* **582**, 1251–1262 (2003)
- [27] K. Fraval, F. Gunsing et al., *Phys. Rev. C* **89**, 044609 (2014)
- [28] R. L. Macklin, R. R. Winters, *Astrophys. J.* **208**, 812 (1976)
- [29] C. Domingo-Pardo, *First measurement of the s-process branching  $^{79}\text{Se}(n,\gamma)$* , CERN-INTC-2014-005 / INTC-I-155
- [30] B. Alpert et al., *Eur. Phys. J. C* **75**, 112 (2015)